



**HAL**  
open science

## The influence of montmorillonite on the flame-retarding properties of intumescent bio-based PLA composites

Raíssa Carvalho Martins, Simone Pereira da Silva Ribeiro, Regina Sandra Veiga Nascimento, Marco Antonio Chaer Nascimento, Marcos Batistella, J. Lopez-Cuesta

### ► To cite this version:

Raíssa Carvalho Martins, Simone Pereira da Silva Ribeiro, Regina Sandra Veiga Nascimento, Marco Antonio Chaer Nascimento, Marcos Batistella, et al.. The influence of montmorillonite on the flame-retarding properties of intumescent bio-based PLA composites. *Journal of Applied Polymer Science*, 2022, 139 (22), pp.52243. 10.1002/app.52243 . hal-03590670

**HAL Id: hal-03590670**

**<https://imt-mines-ales.hal.science/hal-03590670>**

Submitted on 2 Mar 2022

**HAL** is a multi-disciplinary open access archive for the deposit and dissemination of scientific research documents, whether they are published or not. The documents may come from teaching and research institutions in France or abroad, or from public or private research centers.

L'archive ouverte pluridisciplinaire **HAL**, est destinée au dépôt et à la diffusion de documents scientifiques de niveau recherche, publiés ou non, émanant des établissements d'enseignement et de recherche français ou étrangers, des laboratoires publics ou privés.

# The influence of montmorillonite on the flame-retarding properties of intumescent bio-based PLA composites

Raíssa Carvalho Martins<sup>1,2</sup> Simone Pereira da Silva Ribeiro<sup>1</sup>  
Regina Sandra Veiga Nascimento<sup>1</sup> Marco Antonio Chaer Nascimento<sup>1</sup>  
Marcos Batistella<sup>2</sup> José-Marie Lopez-Cuesta<sup>2</sup>

<sup>1</sup>Instituto de Química, Universidade Federal do Rio de Janeiro, Cidade Universitária, Rio de Janeiro, Brazil

<sup>2</sup>Polymères Composites et Hybrides (PCH), IMT Mines Ales, Ales Cedex, France

## Correspondence

Raíssa Carvalho Martins, Polymères Composites et Hybrides (PCH), IMT Mines Ales, 6, Avenue de Clavières, 30319 Ales Cedex, France.  
Email: raissacarvalho1@gmail.com

## Funding information

Conselho Nacional de Desenvolvimento Científico e Tecnológico, Grant/Award Number: 307924/2019-0; Coordenação de Aperfeiçoamento de Pessoal de Nível Superior, Grant/Award Number: 001; Fundação Carlos Chagas Filho de Amparo à Pesquisa do Estado do Rio de Janeiro, Grant/Award Numbers: E-26/202.939/2017, E-26/201.861/2019, E-26/010.002270/2019; Instituto Nacional de Ciência e Tecnologia em Materiais Complexos Funcionais, Grant/Award Number: CNPq 465452/2014-0

## 1 | INTRODUCTION

Instead of using halogenated composites, an alternative solution for the polymers high flammability is the incorporation of intumescent formulations, which consist of an acid source, a polyhydroxylated carbonaceous compound and a blowing agent. When submitted to high temperatures, these components react producing an expanded carbonaceous layer (char), which acts as a physical barrier, avoiding the interchange of oxygen, heat, and fuel between the material surface and the outside, ceasing the flame.<sup>1</sup> A classical intumescent

## Abstract

Biobased flame-retardant polylactic acid composites were prepared using ammonium polyphosphate (AP), lignin, and a raw montmorillonite (ANa) as the intumescent formulation. The concentration of AP and of ANa was varied in order to study its influence on the flammability properties of the composites. The samples were submitted to cone calorimeter test, thermogravimetric analysis coupled to Fourier-transform infrared spectroscopy (TGA-FTIR), limiting oxygen index (LOI), and UL-94 vertical burn. The cone calorimeter residues were analysed through scanning electronic microscopy, X-ray diffraction, and FTIR. The results show that the combined addition of the intumescent formulation and the ANa leads to an improvement in the fire behavior of the composites, compared with that of the neat polymer. The best fire-retardant performance was achieved by using the highest AP concentration (17%) and the lowest ANa concentration (1.2%), reaching a LOI value of 39%.

## KEYWORDS

biopolymers and renewable polymers, clay, composites, flame retardance

formulation employed in the literature consists of pentaerythritol (PER) as the polyhydroxylated carbonaceous compound and ammonium polyphosphate (AP), which acts simultaneously as the acid source and the blowing agent.<sup>1,2</sup>

Intumescent formulations can be used in various polymers, including the bio-based ones.<sup>3–8</sup> Among them, polylactic acid (PLA), a compostable thermoplastic originated from renewable carbohydrate sources, such as starch and sugarcane,<sup>9</sup> has shown to be a promising option for many applications.<sup>8</sup> Moreover, some applications need materials with an increased fire resistance. In

order to improve the flame retardancy of PLA, some works in literature evaluated the use of expandable graphite,<sup>9,10</sup> aluminium hydroxide,<sup>11</sup> natural fibers,<sup>9,12</sup> and intumescent formulations.<sup>13</sup> Among these systems, the use of bio-based intumescent formulations with lignin,<sup>13–16</sup> phytic acid,<sup>17</sup> and starch<sup>13</sup> have attracted great attention. Lignin, a residue from the paper and cellulose industry and the second most abundant terrestrial polymer after cellulose, is an attractive candidate to replace PER, as it is a highly cross-linked polyphenolic polymer rich in aliphatic and aromatic carboxylic groups.<sup>13,14</sup> Besides, due to its aromatic structure and good thermal stability it possesses a high ability for char formation.<sup>18</sup> Réti et al.<sup>13</sup> evaluated the efficiency of different intumescent formulations – AP/PER, AP/lignin, and AP/starch – in a PLA matrix, obtaining a high flame retardancy performance for the biobased composites, with a lower heat release and a higher final residue compared with the ones containing AP/PER. Cayla et al.<sup>16</sup> prepared an intumescent PLA textile containing lignin and AP with remarkable flame-retarding properties. Carretier et al.<sup>15</sup> observed synergistic effects on the cone calorimetry tests for PLA composites containing only AP and lignin as the intumescent formulation when the AP/lignin ratio is up to three.

In order to enhance the flame-retardant properties, some works in the literature report the use of synergists in the intumescent PLA compositions, such as organo-modified montmorillonite (Cloisite 30B),<sup>8,19,20</sup> multiwalled carbon nanotubes,<sup>19</sup> expandable graphite,<sup>10</sup> and modified layered double hydroxides,<sup>17</sup> which exhibited better performances when compared with the correspondent systems without the synergism agent. According to a previous work,<sup>21</sup> the addition of a raw montmorillonite, that is, a non-organomodified montmorillonite – to an intumescent polypropylene composite promotes a synergistic effect with the intumescent formulation (composed by AP and PER), improving the flammability properties. For this reason, it is important to evaluate the effect of the addition of a raw montmorillonite on the flame-retarding properties of intumescent PLA composites. Moreover, to the best of our knowledge, there is no study involving the use of raw montmorillonite in an intumescent biobased PLA composite containing ammonium polyphosphate and lignin. Therefore, the aim of this work is to evaluate the impact of the addition of a raw montmorillonite in an unprecedented intumescent formulation—composed of AP, lignin and montmorillonite—on the flame-retardancy of PLA biocomposites.

In order to evaluate the flammability of the composites, they were submitted to cone calorimetry, limiting oxygen index (LOI), and UL-94 vertical burn tests. The thermal behavior was analysed through thermogravimetric analysis coupled to FTIR (TGA-FTIR). In addition,

scanning electronic microscopy (SEM), X-ray diffraction (XRD), and FTIR were employed for the analyses of the cone calorimeter residues.

## 2 | EXPERIMENTAL

### 2.1 | Materials

The raw sodic montmorillonite (ANa) was provided by Bentonisa Bentonita do Nordeste S.A. (Paraíba, Brazil). Ammonium polyphosphate (AP) was purchased from Clariant under the trade name Exolit AP 422; alkaline lignin (LIG) was supplied by Tokyo Chemical Industry (product code L0082) and polylactic acid (PLA), by NatureWorks under the trade name Ingeo™ Biopolymer 2003D.

### 2.2 | Montmorillonite characterization

The chemical composition, the crystallinity, the textural properties, and the particle size analysis of the ANa sample have been presented in a previous work.<sup>21</sup>

### 2.3 | Processing of the composites

PLA, AP, LIG, and ANa were used to prepare the polymeric composites. The concentration of LIG was kept constant while the ones of AP and ANa were varied, as shown in Table 1. The relative amounts of the materials used to prepare the composites were based upon some assumptions. According to Carretier et al.,<sup>15</sup> a synergistic effect in the fire performance is observed when a ratio of AP/lignin equal or higher than 3 is used in the intumescent formulation, and the best performance is obtained for the composite containing 80% PLA + 17% AP + 3% lignin. From the literature,<sup>22</sup> it is known that, for AP/PER systems, the optimum proportion for intumescent systems is 3AP:1PER. In a previous work<sup>21</sup> which evaluated the

TABLE 1 Relative concentration (in % m/m) of PLA and additives for each composite produced

Composite	PLA	AP	LIG	ANa
PLA/16AP	81.2%	15.8%	3%	—
PLA/16AP/1ANa	80%	15.8%	3%	1.2%
PLA/16AP/3ANa	78.2%	15.8%	3%	3%
PLA/17AP	80.0%	17%	3%	—
PLA/17AP/3ANa	77%	17%	3%	3%
PLA/17AP/1ANa	78.8%	17%	3%	1.2%

synergism between AP/PER and montmorillonite in a polypropylene matrix, a 3% of raw montmorillonite synergist was maintained within a proportion of 2.5 PER: 1 montmorillonite. For the current PLA/AP/lignin system, in order to keep the same proportion, a concentration of 1.2% of montmorillonite should be used for 3% of lignin. Therefore, considering all these aspects and keeping the loading around 20% as currently used in the literature for fire-retardant PLA composites,<sup>15</sup> and the lignin concentration constant (3%), a total of six composites were prepared: two of them without montmorillonite (containing 17% and 15.8%AP) and four combining 17% and 15.8 of %AP with 3% and 1.2% of montmorillonite. The effect of the montmorillonite concentration was considered in the works of Chigwada and Wilkie,<sup>23</sup> Martins et al.<sup>21</sup> and Guo et al.<sup>8</sup>

The polymeric materials were processed in a BC21 Clextal 900 mm (Firminy, France) twin screw extruder. The extruder has twelve heating zones that were kept at the following temperatures:  $T_{\text{zone 1}} = 50^{\circ}\text{C}$ ,  $T_{\text{zones 2,3}} = 195^{\circ}\text{C}$ ,  $T_{\text{zone 4}} = 190^{\circ}\text{C}$ ,  $T_{\text{zones 5-12}} = 180^{\circ}\text{C}$ . The materials were fed into zone 1, with a flow rate of  $4 \text{ kg h}^{-1}$  and a thread rotation of 200 rpm. The materials were pelletized in a Scheer pelletizer (Germany) and specimens of  $100^{\circ} \times 100^{\circ} \times 4 \text{ mm}^3$  were prepared using a 50 ton Krauss Maffei (Munich, Germany) injection molding press with mold and screw temperatures of 30 and  $180^{\circ}\text{C}$ , respectively. The raw components were dried overnight before extrusion at  $60^{\circ}\text{C}$  in compressed air Piovan (Italy) dryers. The same procedure was used for the produced pellets before the injection molding step.

## 2.4 | Flammability tests

### 2.4.1 | Cone calorimetry

Cone calorimeter tests were conducted on a fire testing technology (FTT) equipment using an external heat flux of  $50 \text{ kW m}^{-2}$ , a 25 mm-distance between the cone and the sample, and an air flow of  $24 \text{ L s}^{-1}$ . The following parameters were studied: time to ignition (TTI), peak of heat release rate (pHRR), total heat released (THR), maximum average rate of heat emission (MARHE), effective heat of combustion (EHC), and mass ratio of the remaining residue ( $M_{\text{residue}}$ ).

### 2.4.2 | Limiting oxygen index

The limiting oxygen index (LOI, ISO 4589-2) is a quantitative test which enable the determination of the minimum oxygen concentration required for supporting the flame combustion of the specimen placed in upright

position. This test was performed in an apparatus composed by a gas flow controller and a burning chamber with controlled atmosphere, using  $100 \times 7 \times 4 \text{ mm}$  specimens.

A propane flame is approached to the top of the specimen, which should extinguish the flame in less than 3 min without having 50% of its length consumed. The oxygen concentration is gradually increased until the material is no longer able to maintain those conditions. The higher the %  $\text{O}_2$  achieved, the better is the performance of the material.

### 2.4.3 | Underwriters UL-94 test

The self-extinguishing time of the composites was assessed by the Underwriters Laboratory's UL-94 test (vertical burning test; ASTM D 380), in which a 4 mm thickness specimen vertically oriented has its top clamped to a stand and a methane burner is placed directly below it. This test classifies the material based on some parameters, such as the time that the material continues to burn after removal of the heat source after the first ( $t_1$ ) and the second ( $t_2$ ) flame approximation, the incandescence time ( $t_3$ ), the occurrence of burning drips and the burnt extension of the specimen. The highest classification, designated as V0, is given to a material which is able to quickly extinguish the flame and presents a weak afterglow, without burning drips. The lowest classification is V2, given to a material that takes longer to extinguish the flame, or that exhibits burning drips, or which presents both behaviors.

## 2.5 | Scanning electron microscopy of the composites

The inner surface obtained by transversal cryofracture of the composites before being burnt and the surface of the residues obtained at the end of the cone calorimeter test were analysed in a Quanta FEG 200 (FEI Company, Hillsboro, OR, USA) SEM equipment.

## 2.6 | X-ray diffraction of the composites

The X-ray diffractograms of the milled composites before burning and of the surface of the residues obtained at the end of the cone calorimeter test were collected in a Bruker AXS D8 Advance diffractometer using the  $\text{CuK}\alpha$  ( $\lambda = 1.54 \text{ \AA}$ ) line, a Lynxeye detector and a scanning range of  $5^{\circ}$  to  $70^{\circ}$ , during 1 h.

## 2.7 | Fourier transform infrared spectroscopy of the composites

The chemical nature of the residues obtained at the end of the cone calorimeter tests was investigated through a Vertex 70 FT MIR spectrometer (Bruker, Billerica, MA, USA) with a  $4 \text{ cm}^{-1}$  resolution and a spectral range of 4000 to  $400 \text{ cm}^{-1}$ . The analyses were performed using KBr pellets with a sample concentration of 1%.

## 2.8 | Thermogravimetric analysis coupled to gas phase Fourier transform infrared spectroscopy of the composites

The thermal stability was investigated using a SETSYS evolution TGA equipment, from Setaram (Caluire, France), coupled to a gas phase IS10 Thermo IR spectrometer. Samples of 12 mg were analysed on an alumina microbalance pan with a  $10^\circ\text{C min}^{-1}$  heating rate,  $100 \text{ cm}^3 \text{ min}^{-1}$  synthetic air flow and a temperature range of 30 to  $900^\circ\text{C}$ . In order to evaluate the influence of the additives on the thermal stability of the composites, experimental, and theoretical mass loss curves were compared. To construct the theoretical curves, firstly, each constituent of the composite (PLA, the intumescent formulation, IF, and ANa) had its individual TGA curve measured experimentally. The theoretical mass loss ( $M_{theo} [T]$ ) was then calculated in an ordinary spreadsheet, considering the contribution of each additive in its respective concentration in the composite, as shown in Table 2. The theoretical mass loss of the intumescent formulation as function of the temperature,  $M_{IF} (T)$ , was calculated based on the experimental TGA curve of a mixture of AP and lignin with the same concentrations used in the composites, as shown in Table 1. This procedure allows the thermal effect of possible reactions between AP and lignin to be considered in the calculations, opening the possibility of establishing the individual effect of the clay addition.

## 3 | RESULTS AND DISCUSSION

### 3.1 | Cone calorimetry

The CC tests were designed to investigate, separately, the effect of the ammonium polyphosphate (% AP) and of the montmorillonite (% ANa) concentrations on the fire-retardant properties of the composites. Table 3 presents the values of the time to ignition (TTI), the peak of heat release rate (pHRR), the total heat released (THR), the maximum average rate of heat emission (MARHE) as a function of time, the effective heat of combustion (EHC) and the mass ratio of the remaining residue ( $M_{\text{residue}}$ ). The %  $M_{\text{residue}}$  was calculated according to Equation 1:

$$\%M_{\text{residue}} = \frac{M_f(g)}{M_i(g)} \times 100 \quad (1)$$

where  $M_i$  and  $M_f$  stand for the initial and final mass of the sample.

The EHC was calculated according to Equation 2:

$$\text{EHC} (\text{MJ kg}^{-1}) = \frac{0.0083 \text{ m}^2}{(M_i - M_f) \text{ kg}} \times \text{THR} (\text{MJ m}^{-2}) \quad (2)$$

where  $0.0083 \text{ m}^2$  stands for the exposed surface area of the sample.

The samples without ANa (pristine PLA, PLA/16AP, and PLA/17AP) were analysed in order to investigate the influence of the addition of the intumescent formulation to the PLA matrix, as well as the effects of varying the concentration of ammonium polyphosphate while keeping constant the concentration of lignin. According to Figure 1a, PLA degrades in a single step with a pHRR of  $499 \text{ kW m}^{-2}$ . The addition of the intumescent formulation did not change significantly the TTI values, but it promoted significant reductions of the pHRR (by 45% for PLA/16 AP and 47% for PLA/17AP) and of the THR (by 26% for PLA/16AP and 36% for PLA/17AP) values

TABLE 2 Equations used to construct the mass loss theoretical curves for each composite

Composite	$M_{\text{theo}} (T)$
PLA/16AP	$M_{\text{theo}} (T) = 0.812 M_{\text{exp,PLA}} (T) + 0.188 M_{\text{exp,IF}} (T)$
PLA/16AP/1ANa	$M_{\text{theo}} (T) = 0.80 M_{\text{exp,PLA}} (T) + 0.188 M_{\text{exp,IF}} (T) + 0.012 M_{\text{exp,ANa}} (T)$
PLA/16AP/3ANa	$M_{\text{theo}} (T) = 0.782 M_{\text{exp,PLA}} (T) + 0.188 M_{\text{exp,IF}} (T) + 0.03 M_{\text{exp,ANa}} (T)$
PLA/17AP	$M_{\text{theo}} (T) = 0.80 M_{\text{exp,PLA}} (T) + 0.20 M_{\text{exp,IF}} (T)$
PLA/17AP/3ANa	$M_{\text{theo}} (T) = 0.77 M_{\text{exp,PLA}} (T) + 0.20 M_{\text{exp,IF}} (T) + 0.03 M_{\text{exp,ANa}} (T)$
PLA/17AP/1ANa	$M_{\text{theo}} (T) = 0.788 M_{\text{exp,PLA}} (T) + 0.20 M_{\text{exp,IF}} (T) + 0.012 M_{\text{exp,ANa}} (T)$

Note:  $M (T)$ : experimental mass loss as function of the temperature, T.  $M_{IF} (T)$  was calculated based on the TGA curve of the mixture of AP and lignin at the same proportion used for each composite, as described in Table 1.

TABLE 3 Cone calorimeter results obtained for the produced composites

Sample	TTI (s)	pHRR ( $\text{kW m}^{-2}$ )	THR ( $\text{MJ m}^{-2}$ )	MARHE ( $\text{kW m}^{-2}$ )	$M_{\text{residue}}$ (%)	EHC ( $\text{MJ kg}^{-1}$ )
PLA	38	499	95	302	0	16.1
PLA/16AP	35	272	70	186	20	13.6
PLA/16AP/1ANa	35	254	69	167	23	13.8
PLA/16AP/3ANa	33	248	77	197	20	16.0
PLA/17AP	32	264	61	164	28	13.1
PLA/17AP/1ANa	36	233	58	131	32	13.0
PLA/17AP/3ANa	34	237	75	187	20	14.2

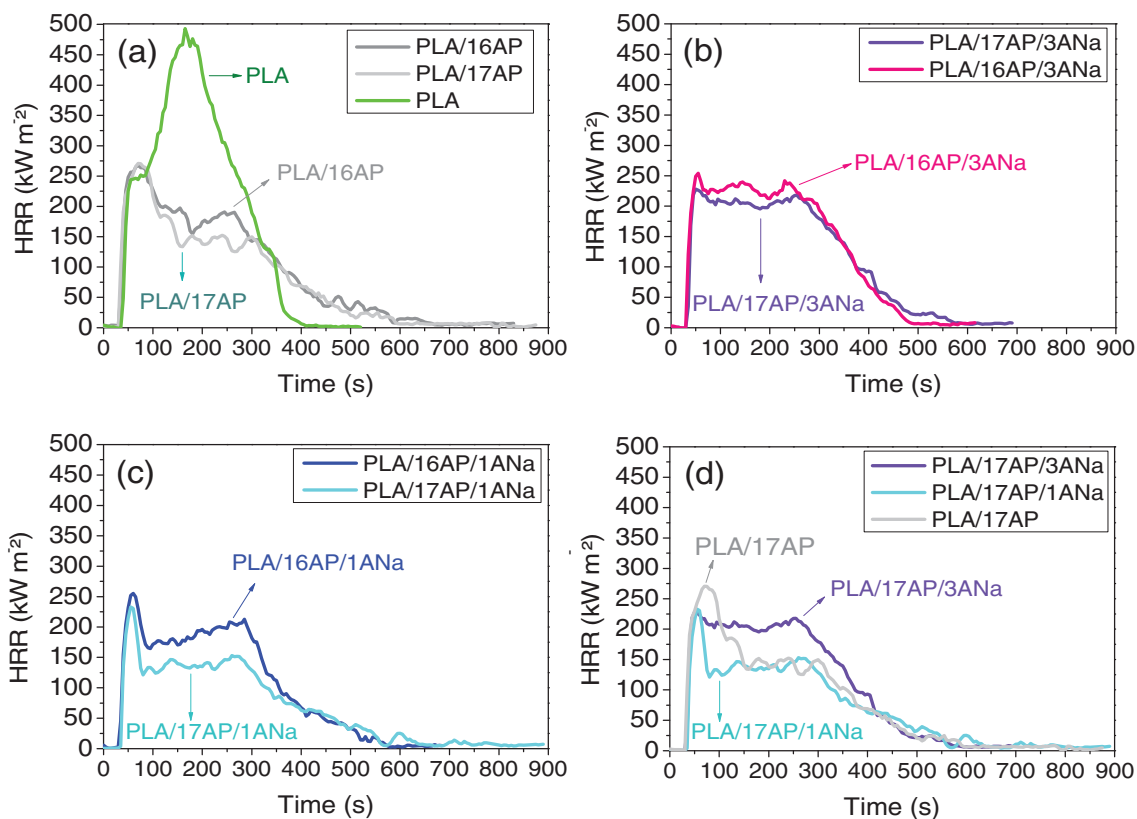


FIGURE 1 HRR curves for (a) PLA and composites without ANa; (b) composites with 3% ANa; (c) composites with 1% ANa; (d) composites with 17% AP [Color figure can be viewed at [wileyonlinelibrary.com](http://wileyonlinelibrary.com)]

when compared with those for the neat PLA. Furthermore, the EHC decreased from 16.1 (PLA) to 13.6  $\text{MJ Kg}^{-1}$  for the PLA/16AP and to 13.1  $\text{MJ Kg}^{-1}$  for the PLA/17AP composites, and the MARHE values decreased by 38% for the PLA/16AP and by 46% for PLA/17AP composites. Also noticeable are the ratios of remaining residues (20% for PLA/16AP and 28% for PLA/17AP) evidencing the formation of a charred structure.

Another interesting point is the change in the HRR curve profiles of PLA and the composites (Figure 1). Although the curves are almost overlapped during the first 100 s of testing, for longer times the formation of a

surface protective layer avoids the complete degradation of the intumescent composites, as observed for the neat PLA (Figure 1a), lowering the HRR to an almost constant value until approximately 300 s. Although the PLA/16AP and the PLA/17AP composites present identical HRR curves profiles (Figure 1a), the latter exhibits a lower THR, as previously mentioned.

Figure 1b presents the HRR variation as a function of time for the systems containing 3% ANa. It is noticeable the change in the curve profiles when compared with the systems without clay (Figure 1a). The addition of 3% ANa promotes only a slight decrease in the HRR values after

the pHRR, leveling off the curves to 200 and 250 kW m<sup>-2</sup> until around 300 s of testing. This behavior can be related to a poor quality of the formed surface protective layer, which is not able to protect well the polymeric material and to prevent the mass and the heat transfer. Both the PLA/17AP/3ANa and PLA/16AP/3ANa composites present higher THR values than their corresponding composites without ANa, indicating that the addition of that amount of montmorillonite is not convenient to improve the fire-retardant properties in the cone calorimeter. Also, the PLA/16AP/3ANa and PLA/17AP/3ANa composites present higher EHC values than the corresponding ones without clay, PLA/16AP, and PLA/17AP.

The plots for the composites containing 1.2% of ANa (PLA/16AP/1ANa and PLA/17AP/1ANa) are presented in Figure 1c. They exhibit the same profile, but the HRR values for PLA/17AP/1ANa curve are clearly lower than the ones for PLA/16AP/1ANa after the pHRR. It also presents a higher % residue indicating that it could be more advantageous to use 17% than 15.8% of AP for this system. Also, the MARHE values for both composites are lower than the corresponding ones for the composites without clay. The TTI values do not vary significantly with the addition of ANa.

The HRR plots in Figure 1c clearly show that for the composites containing 1.2% of ANa there is a sharp decrease in the HRR after the pHRR, followed by a stable plateau (around 125–150 kW m<sup>-2</sup> for PLA/17AP/1ANa and 175–200 kW m<sup>-2</sup> for PLA/16AP/1ANa) until 300 s of testing. This behavior indicates that a more resistant surface protective layer could be formed under these conditions, reducing the heat and mass transfer. On the other hand, the HRR plots for the composites with 3% of ANa (Figure 1b) show a slight reduction of the HRR just after the pHRR, followed a plateau around 200–250 kW m<sup>-2</sup>. The increase from 1.2% to 3% of montmorillonite could lead to a more brittle surface layer, favoring the mass transfer with the external environment. These results show that the concentration of ANa plays an important role in promoting the changes observed in the profiles of the HRR curves.

From the previous results, it is possible to conclude that, among all the composites studied, the best performance in the CC tests is achieved with the addition of 17% ammonium polyphosphate. Figure 1d shows the HRR plots for all the composites containing 17% of AP and different contents of ANa. From Figure 1d and the results in Table 3, it is clear that all together the material containing 1.2% of ANa shows the best performance, reducing the pHRR and the MARHE values and producing the highest amount of residue (32%) at the end of the test.

## 3.2 | Limiting oxygen index

According to the LOI test results (Figure 2), the addition of clay to the intumescent formulation increased significantly the LOI values for all the systems, improving the flame-retarding properties of the montmorillonite-containing composites. For the systems containing 17% of ammonium polyphosphate the LOI result reached 39% compared with the LOI of 30% for the reference system without clay, PLA-17AP. The value of 39% is higher than those of similar systems reported in the literature. Zhang et al.<sup>24</sup> observed LOI values from 29.5% to 35.5% for composites containing PLA, microencapsulated ammonium polyphosphate, lignin and 2% of organic modified montmorillonite. For the systems containing 15.8% of AP and ANa, the LOI value increased by 6 and 8 units when compared with PLA/16AP, reaching 35 and 37% O<sub>2</sub>. The best performance in the LOI test was achieved by the composites with clay containing 17% of AP.

## 3.3 | UL-94

The results obtained in UL-94 tests are summarized in Table 4. The pristine PLA did not classify. Although the composites were able to extinguish the flame very quickly (in less than 50 s, as V-0 materials), all of them presented dripping with ignition of the cotton wool, which characterizes a V-2 material. This result shows that the addition of the montmorillonite did not affect the performance of the intumescent composites in the UL-94. Zhang et al.<sup>14</sup> produced PLA composites (3 mm-thickness) containing AP combined with lignin or urea-modified lignin in different proportions maintaining a 23% loading. All the composites achieved the V-2 classification, except for the one with the weight ratio of 4 AP: 1 urea-modified lignin, which achieved the V-0 classification. Réti et al.<sup>13</sup> produced

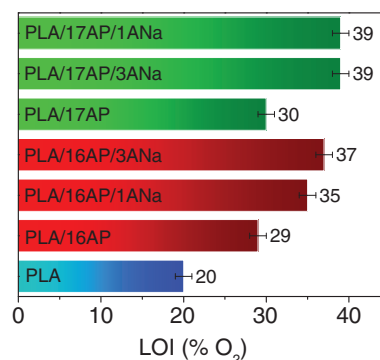


FIGURE 2 Results of LOI tests for the composites studied. The values are in % ± 1 [Color figure can be viewed at [wileyonlinelibrary.com](http://wileyonlinelibrary.com)]

TABLE 4 Results of the UL-94 tests

Sample	( $t_1 + t_2$ ) for the 5 specimens (s)	$t_3$ for the 5 specimens (s)	Dripping with cotton ignition	Specimens burned in all their extension	Classification
PLA	246	—	Yes	Yes	Not classified
PLA/16AP	24	—	Yes	No	V-2
PLA/16AP/1ANa	8	4	Yes	No	V-2
PLA/16AP/3ANa	13	—	Yes	No	V-2
PLA/17AP	25	—	Yes	No	V-2
PLA/17AP/3ANa	15	—	Yes	No	V-2
PLA/17AP/1ANa	16	—	Yes	No	V-2

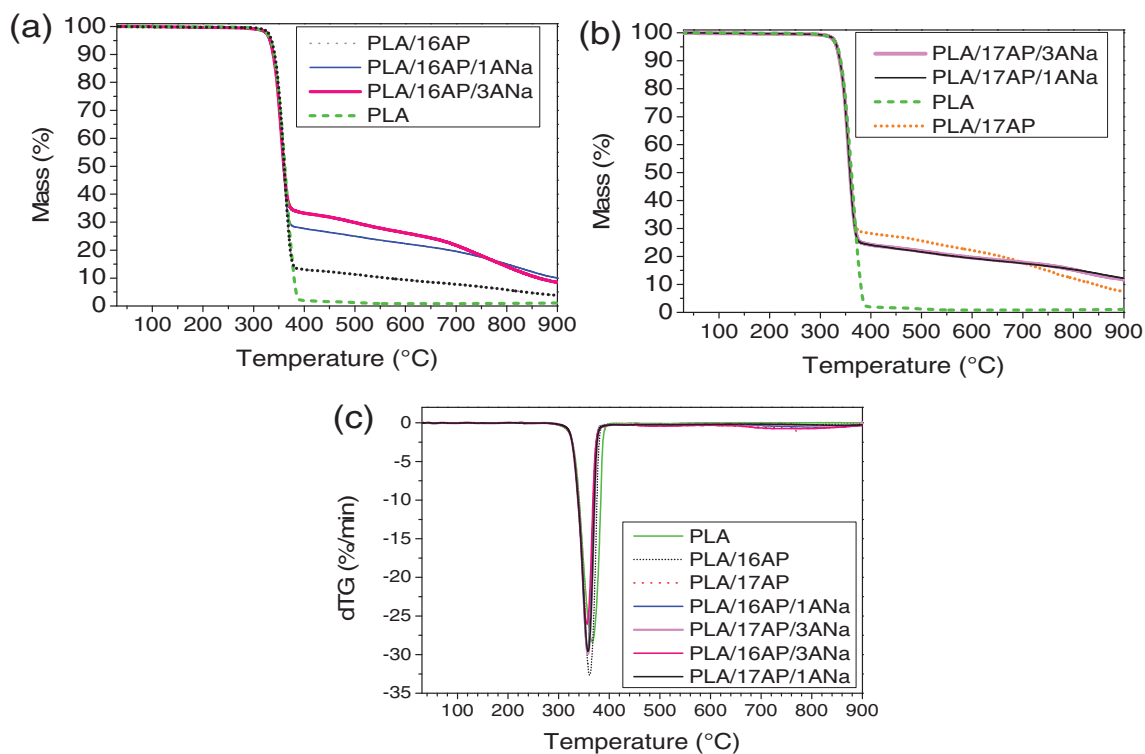
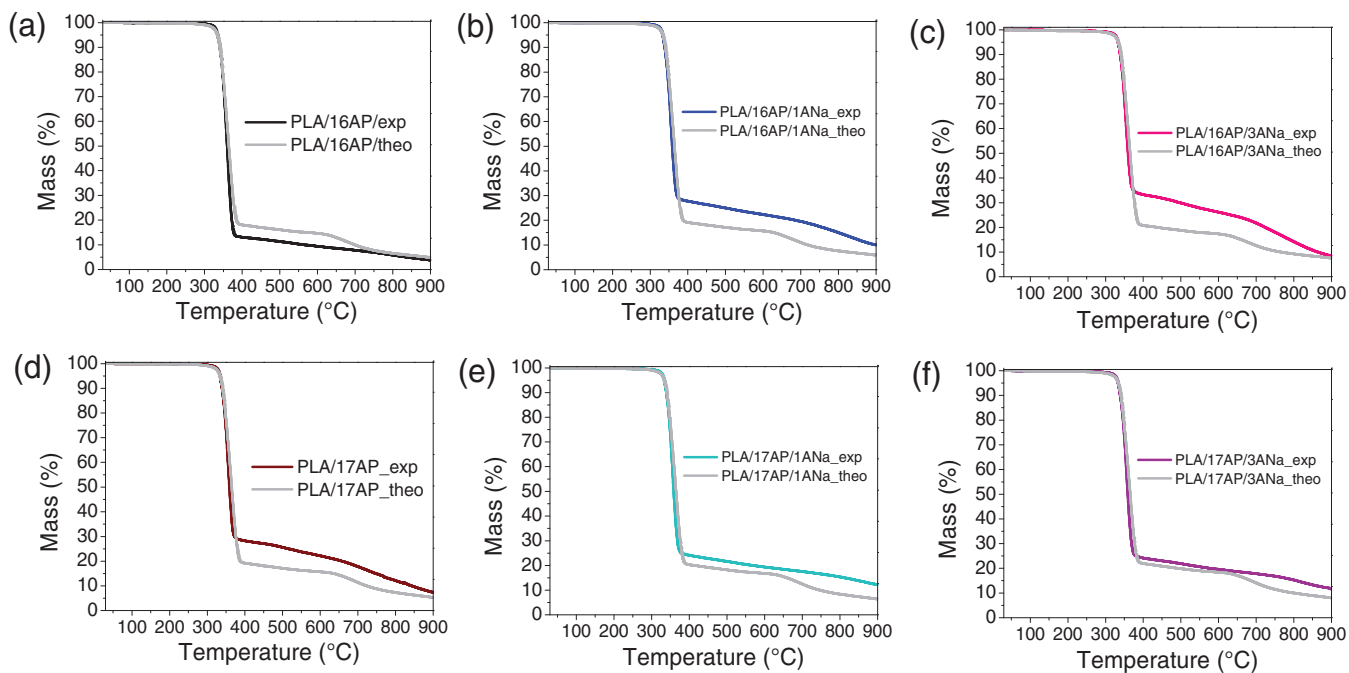


FIGURE 3 (a) Experimental TGA curves for PLA and the composites containing 15.8% AP; (b) experimental TGA curves for composites containing 17% AP; (c) experimental dTG curves for PLA and all the composites [Color figure can be viewed at wileyonlinelibrary.com]

TABLE 5 TGA and dTG data for PLA and the produced composites

Sample	$T_{\text{onset}}$ (°C)	$T_{\text{dTG peak}}$ (°C)	Experimental residue at 900°C (% mass)	Theoretical residue at 900°C (% mass)
PLA	324	366	0	—
PLA/16AP	316	355	3.8	4.9
PLA/16AP/1ANa	325	357	10.0	5.9
PLA/16AP/3ANa	323	356	8.5	7.5
PLA/17AP	318	358	7.4	5.3
PLA/17AP/1ANa	324	366	12.2	6.4
PLA/17AP/3ANa	320	359	11.9	8.0



**FIGURE 4** Experimental TGA and dTG curves and comparison with theoretical TGA curve for (a) PLA/16AP; (b) PLA/16AP/1ANa; (c) PLA/16AP/3ANa; (d) PLA/17AP; (e) PLA/17AP/1ANa; (f) PLA/17AP/3ANa [Color figure can be viewed at [wileyonlinelibrary.com](https://onlinelibrary.wiley.com)]

composites (3 mm-thickness) containing higher proportions of AP and lignin: 60% PLA + 30% AP + 10% lignin which classified as V-0.

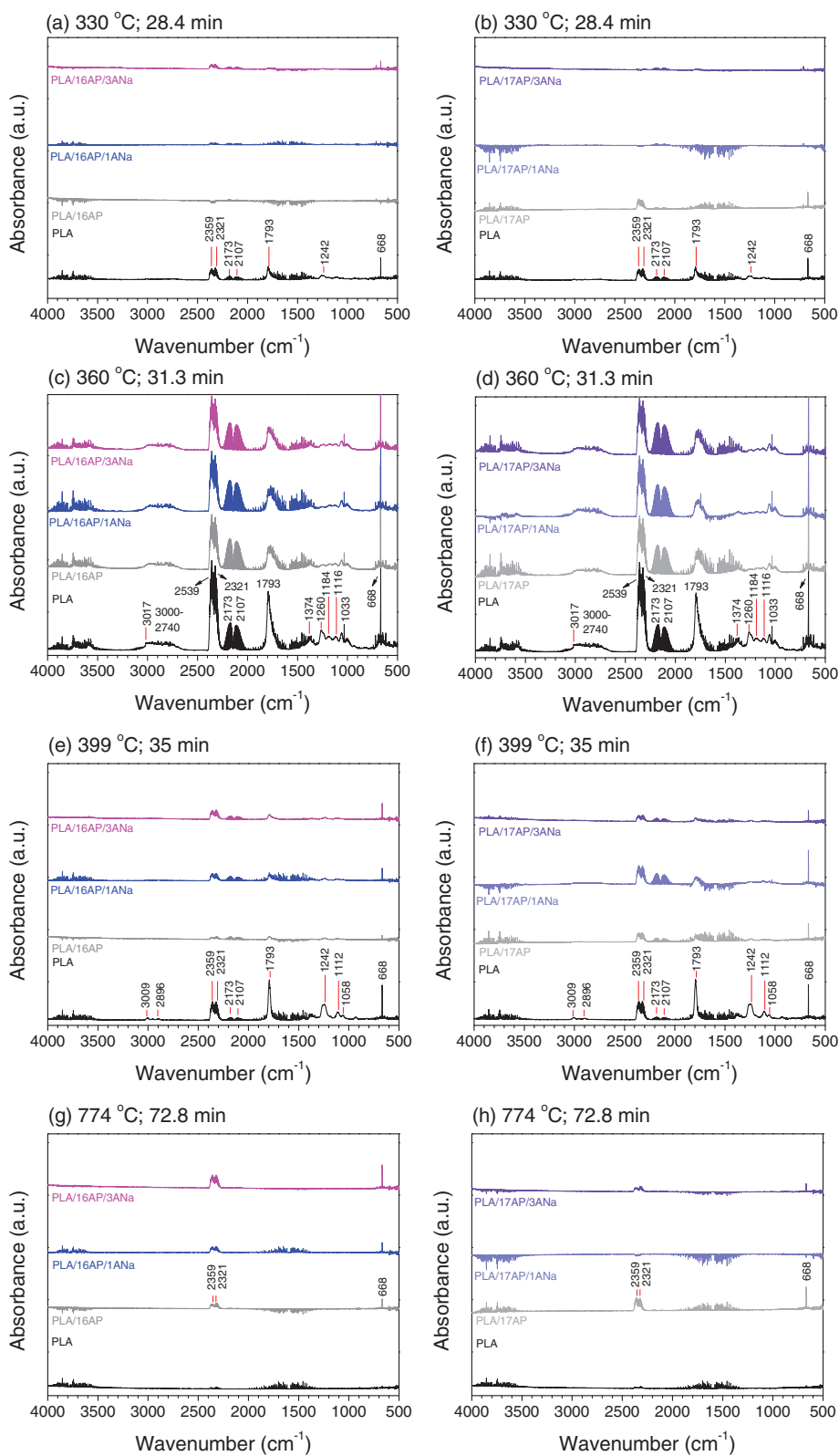
### 3.3.1 | TGA results

The experimental TGA and dTG curves for PLA and the composites containing 15.8% and 17% ammonium polyphosphate are presented in Figure 3a-c. Until around 370°C the curves are almost overlapped with the PLA curve, with very similar values of  $T_{\text{onset}}$  (see Table 5). While the PLA thermal degradation occurs in a single step between 300 and 370°C, the composites containing the intumescent formulation exhibit a very different profile for temperatures above 370°C, with more than one degradation step. Until 370°C the mass loss is related to the degradation of the polymeric matrix and the additives: lignin starts to degrade around 230°C<sup>16</sup> and the ammonium polyphosphate releases ammonia around 330°C.<sup>16</sup> The products of degradation in the condensed phase give rise to more thermally stable products at 370°C than the neat PLA, leading to a better thermal stability of the material and a greater amount of residue at 900°C. According to Figure 3a, the addition of montmorillonite increases the thermal stability of the composites along all the temperature range of 370–900°C when compared with that of the composite without clay (PLA/16AP), increasing the final residue by a factor higher than 2. It is interesting to

observe that a lower amount of the ANa montmorillonite (PLA/16AP/1ANa) leads to a higher final residue (10% against 8.5% for PLA/16AP/3ANa). A different behavior is observed for the formulations containing 17% of APP (Figure 3b). Between 400 and 700°C the composite without ANa (PLA/17AP) presents a lower mass loss compared with the formulations containing montmorillonite. However, for temperatures higher than 700°C, the mass loss ratio for the composites PLA/17AP/3ANa and PLA/17AP/1ANa is almost the same, whereas it decreases faster for the PLA/17AP, reaching about 7.4% of residue at the end of the test. For the system containing 17% of ammonium polyphosphate, the addition of clay seems to be essential to enhance the thermal stability of the materials at temperatures above 700°C. The decrease of the mass loss could be related to the formation of more thermally stable products, such as aluminosilicophosphate species,<sup>25,26</sup> due to some interaction between the clay and AP. The PLA/17AP/1ANa composite presents a final residue slightly higher than that of the PLA/17AP/3ANa, even with a lower mineral content.

Comparing the residues at 900°C in Table 5 it is possible to observe that the values obtained for all the systems containing 17% of AP are superior to the corresponding ones with 15.8% of AP. Moreover, for the same content of ammonium polyphosphate, the residues of the systems with 1.2% of ANa are higher than the ones with 3%, corroborating the best performance observed for the PLA/17AP/1ANa composite in the cone calorimeter tests.

**FIGURE 5** FTIR spectra of gases released during the TGA analysis under synthetic air atmosphere of PLA and the intumescent composites at (a-b) 330°C; (c-d) 360°C; (e-f) 500°C; (g-h) 774°C [Color figure can be viewed at [wileyonlinelibrary.com](http://wileyonlinelibrary.com)]



In order to verify the enhancement of the thermal stability of the composites due to the additives, the experimental and theoretical TGA curves for each system were individually compared in Figure 4a–f. The values of the theoretical residues at 900°C are listed in Table 5. Except

for the PLA/16AP system, the experimental curves indicate that all the other composites exhibit a higher thermal stability, that is, a slower mass loss ratio than the ones predicted theoretically, in the range of 370–900°C. The addition of montmorillonite did not change the

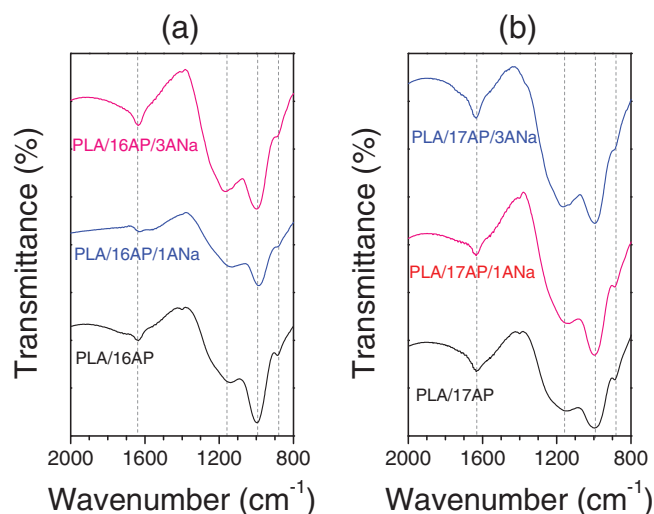


**FIGURE 6** FTIR spectra of the chars resulting from the cone calorimeter test of the composites (a) with 15.8% AP; (b) with 17% AP [Color figure can be viewed at [wileyonlinelibrary.com](http://wileyonlinelibrary.com)]

profile of the curves but increased the thermal stability of the composites from 370°C onwards. The amount of residue obtained from the composites containing ANa is significantly higher than the one predicted theoretically. The largest variations are observed for the composites containing 1.2% of montmorillonite (an increase of 41% for PLA/16AP/1ANa and of 47.5% for PLA/17AP/1ANa) and the lowest variations, for the composites containing 3% of montmorillonite (33% for PLA/17AP/3ANa and 12% for PLA/16AP/3ANa).

### 3.3.2 | Gas phase analysis of the volatile degradation products through FTIR

The gaseous products originated from the degradation of PLA and the composites under synthetic air atmosphere were analysed by FTIR spectrometry. These analyses were performed in order to have a better understanding about the degradation products of the intumescent composites, as well as about the possible influence of the montmorillonite on the degradation process in the gaseous phase. Moreover, it enables to make a correlation amidst the products generated in the gaseous phase with the measured flame-retarding properties. The spectra at selected temperatures and their respective times of analysis are shown in the Figure 5a-h. The following temperatures were chosen: 330°C (close to the  $T_{\text{onset}}$ ; Table 5); 360°C (close to the dTG peaks; Table 5); 399°C (at the end of the first degradation step); 774°C, close to the degradation temperature of the intumescent layer.

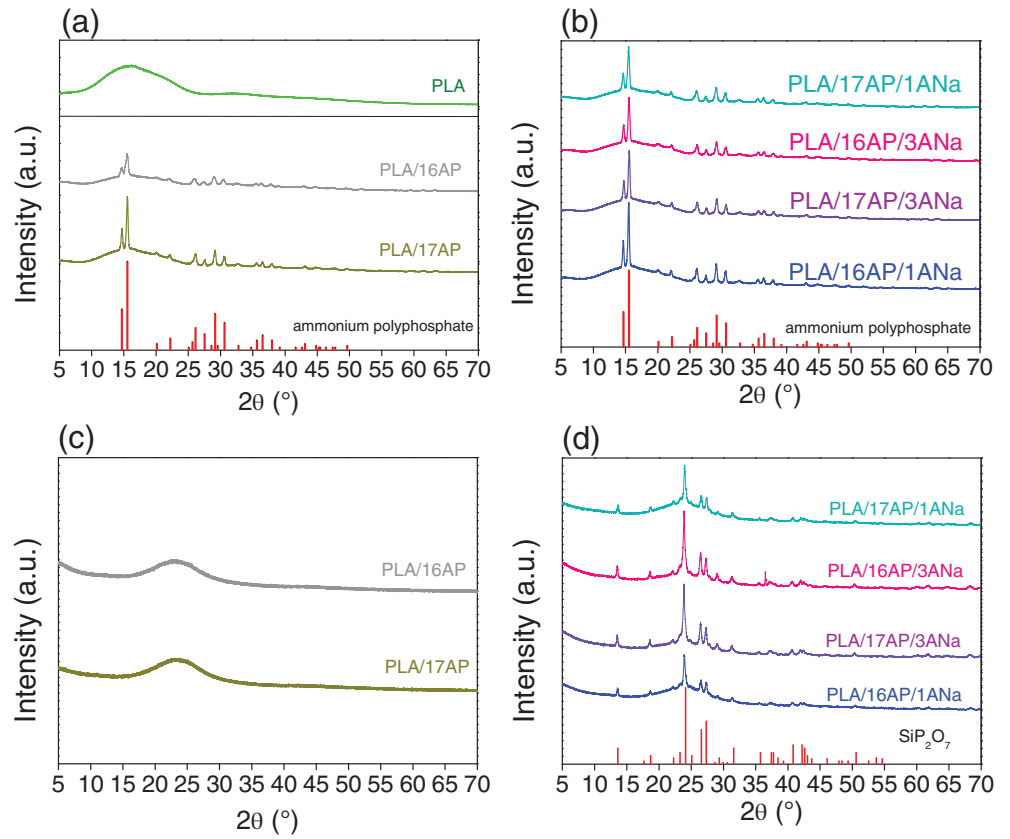
At 330°C ( $T_{\text{onset}}$ ), the PLA spectrum presents bands due to CO<sub>2</sub> (2359, 2321, and 668 cm<sup>-1</sup>)<sup>27-29</sup> and CO (2173

and 2107 cm<sup>-1</sup>).<sup>28,29</sup> The band at 1793 cm<sup>-1</sup> is typical of carbonyl-containing compounds such as lactic acid (“Lactic acid,” 2018),<sup>30</sup> an expected product from the hydrolysis of PLA.<sup>31,32</sup> Bands in the region of 1300–1000 cm<sup>-1</sup> are associated to C–O stretching vibrations in alcohols and esters.<sup>33</sup> A comparison of the PLA spectrum with the ones for the composites containing 15.8% of AP (Figure 5) and 17% of AP (Figure 5b) shows that only the PLA/16AP/3ANa and PLA/17AP composites present some significant bands of CO<sub>2</sub> and CO, but of much lower intensity than the ones in the spectrum of PLA. The other samples do not present distinguishable bands from the baseline. This result shows that at 330°C the neat PLA degrades much faster than the intumescent composites. At 360°C (the temperature of the dTG peak,  $T_{\text{dTG}}$  peak, Table 5), the bands previously observed are intensified (Figure 5c,d) for all the samples, indicating a higher concentration of the degradation products. Besides, new bands are observed, such as the ones at 3017 cm<sup>-1</sup> (alkene C–H stretching vibrations) and in the range of 3000–2740 cm<sup>-1</sup> (alkanes C–H stretching vibrations). The narrow band at 1033 cm<sup>-1</sup> and the two side bands at 1000 and 1060 cm<sup>-1</sup> is assigned to the C–O bond of methanol. The C–O–H bending vibration in alcohols is coupled to H–C–H bending one, producing broad bands in the range of 1440–1220 cm<sup>-1</sup>. However, these bands are usually obscured by the strong CH<sub>3</sub> bending band at 1375 cm<sup>-1</sup><sup>33</sup> (1374 cm<sup>-1</sup> in the present case). The formation of carbonyl and alcohol compounds reveals that the degradation process consists mainly of the breaking of PLA ester bonds. It is also worth noticing that, although the composites spectra present the same bands as the PLA one, their intensity is overall weaker, showing that the degradation process is more intense in the neat PLA than in the intumescent composites. In addition, no difference in the products formed or in the intensity of the bands were observed for the composites, indicating that, up to this point (at 360°C), they all undergo the same thermal degradation process.

At 399°C (Figures 5e,f), the PLA is almost completely consumed, justifying the disappearance of some bands in the region of 1260–1000 cm<sup>-1</sup> (methanol at 1033 cm<sup>-1</sup>) and in the 3000–2740 cm<sup>-1</sup> region (alkanes C–H stretching vibrations), as well as the abruptly reduction in the intensity of the remaining bands. The increase in the thermal stability of the intumescent composites at 399°C (Figure 3) and the lower-intensity bands relative to PLA evidences the formation of the intumescent layer (char), which acts as a physical barrier avoiding the exchange of the volatile products with the external environment.

At 774°C (Figures 5g,h), PLA is completely consumed (according to Figure 3) and no significant bands are observed. For the composites, only the CO<sub>2</sub> related bands

**FIGURE 7** Diffractograms of (a) PLA and composites without ANa before burning; (b) composites with ANa before burning; (c) composites without ANa after burning; (d) composites with ANa after burning [Color figure can be viewed at [wileyonlinelibrary.com](http://wileyonlinelibrary.com)]



### Before burn

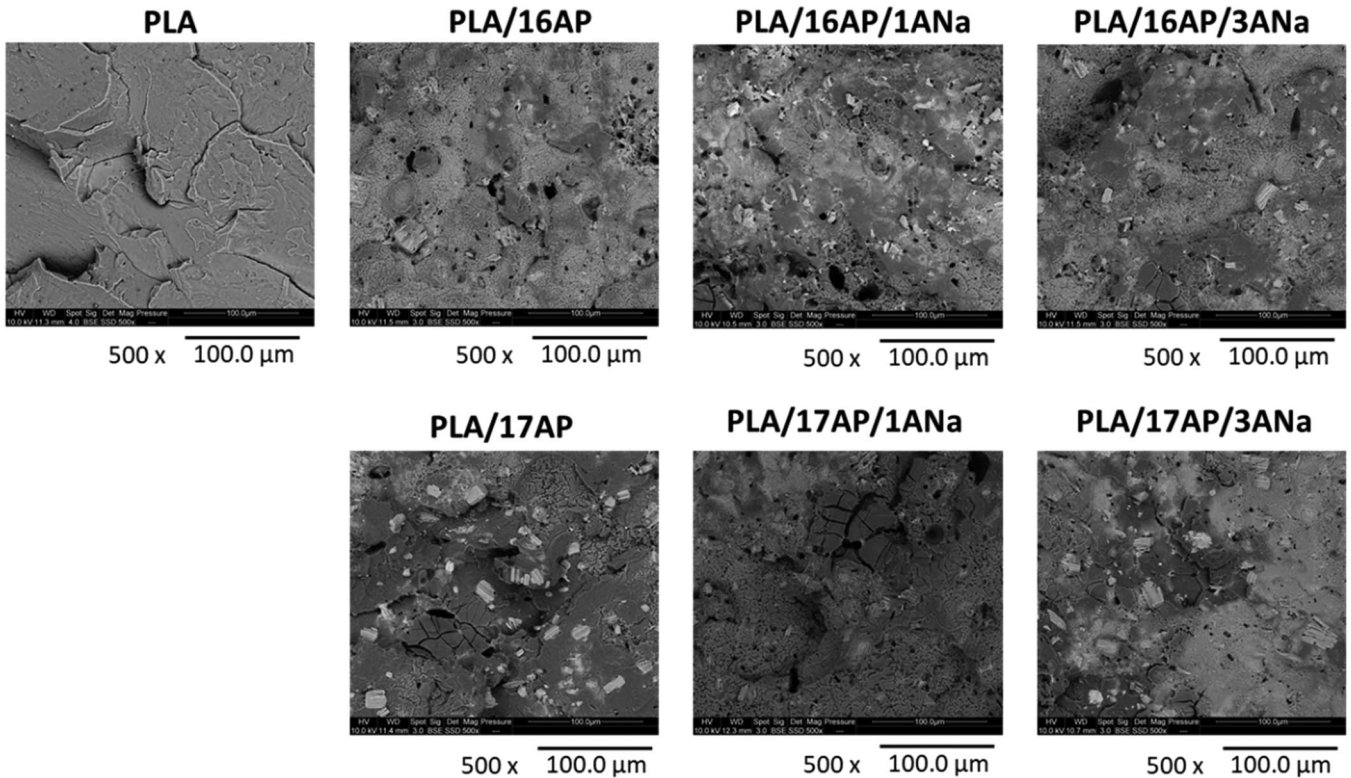
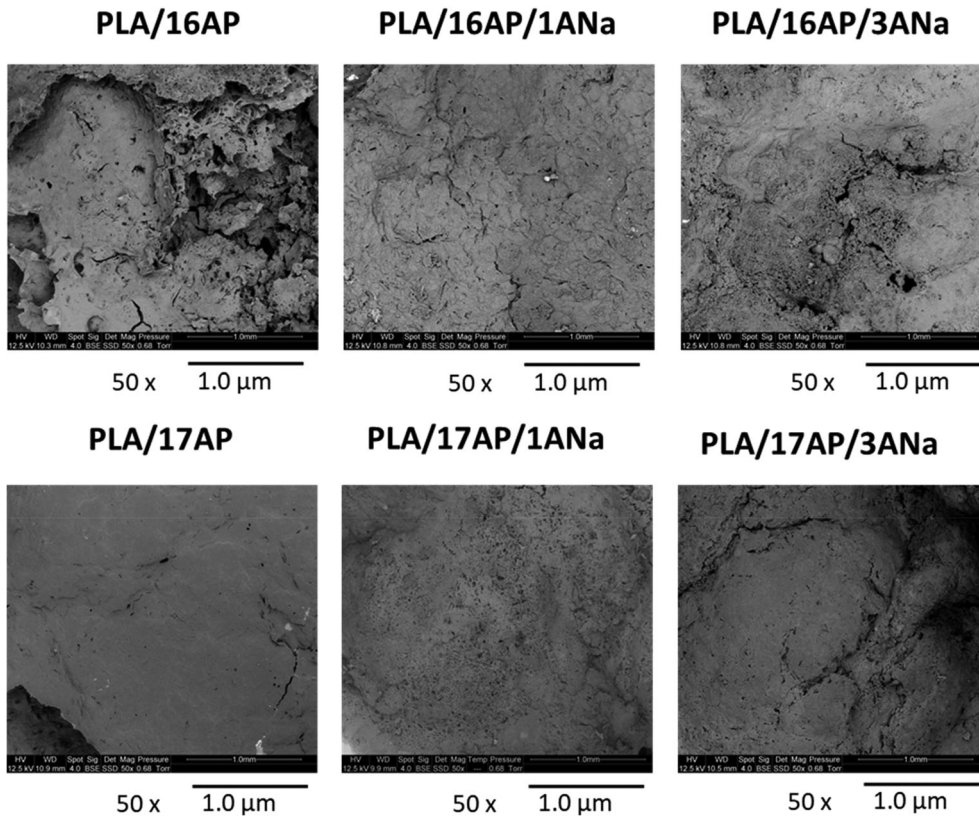


**FIGURE 8** SEM images of (a) PLA and composites before burn, with 500× magnitude

## External surface

FIGURE 9 SEM images of the external surface of the char for each composite, with 50× magnitude



are observed with very low intensities. The PLA/17AP/1ANa composite (1.2% of Mt and 17% of AP), which exhibits the highest amount of residual mass among all the samples (Table 5), shows no bands above the baseline, implying that a very effective char protection layer has been formed.

### 3.3.3 | FTIR spectra of the cone calorimeter residues

The residues obtained after the cone calorimeter tests were analysed through FTIR spectroscopy (Figure 6). According to the literature,<sup>34</sup> the phosphate species and the phosphocarbonaceous structures possibly formed in the char can be characterized in the wavelength range of 850 to 1350  $\text{cm}^{-1}$ . The bands around 886  $\text{cm}^{-1}$  are assigned to the asymmetric vibration of the P—O bond of a P—O—P chain,<sup>34-36</sup> while the ones around 997  $\text{cm}^{-1}$  are referred to the symmetric axial deformation of  $\text{PO}_2$  and  $\text{PO}_3$  in complex carbon phosphates.<sup>34,37</sup> The bands between 1128 and 1167  $\text{cm}^{-1}$  correspond to the stretching mode of P—O—C bonds in phosphate-carbon complexes.<sup>34,35,37</sup> The band around 1635  $\text{cm}^{-1}$  is assigned to C=C stretching vibrations, indicating the formation of unsaturated compounds. These P—O—C and C=C bonds

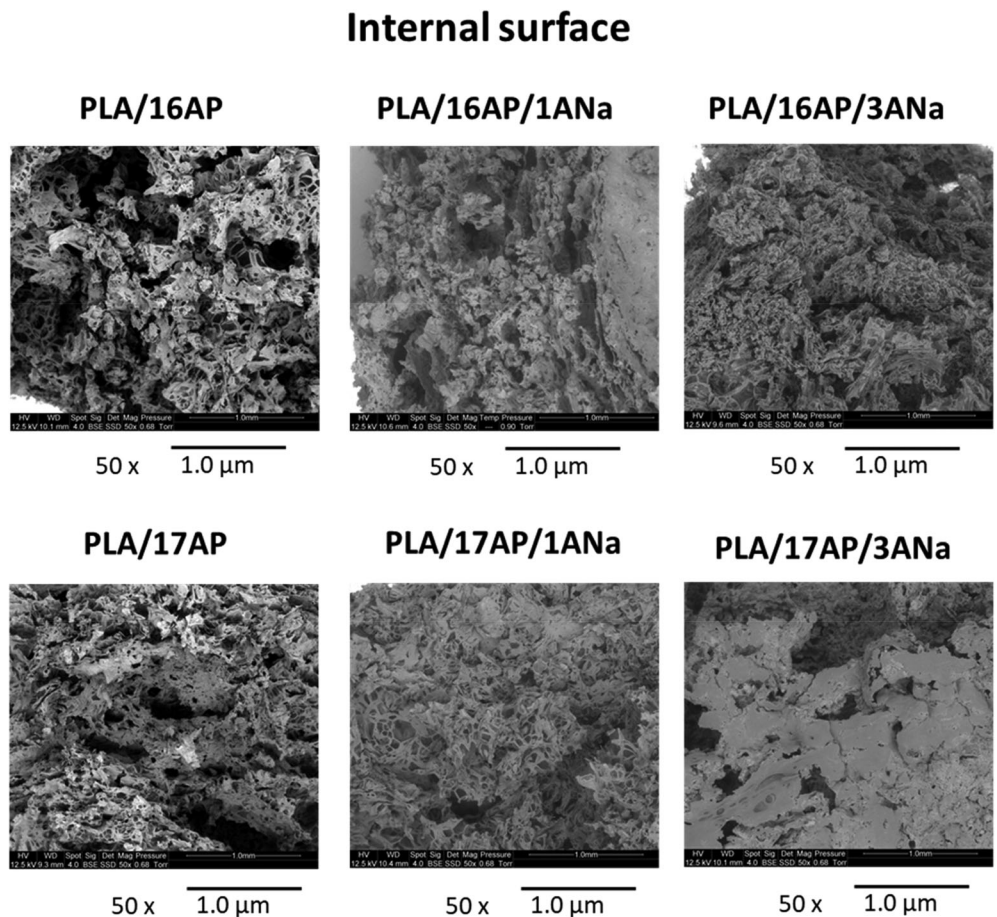
are typical of systems containing an intumescent formulation as they provide a chemical evidence of the intumescent layer formation. Overall, the FTIR spectra of all the char residues do not exhibit significant differences, which is an indication that the composites chars present a very similar chemical composition.

### 3.4 | X-ray diffraction of the composites

Figure 7a-b present the diffractograms of the milled PLA and the composites before being submitted to the cone calorimeter test. PLA shows an amorphous structure, while all the composites exhibit the characteristic reflections of ammonium polyphosphate. As the concentration of montmorillonite is very low, this technique does not allow the identification of the main characteristic reflection of  $2\theta = 6.63^\circ$ <sup>21</sup> for the composites containing clay.

After the cone calorimeter test, the char of each sample was submitted to XRD analysis and their diffractograms are depicted in Figure 7c-d. While PLA/16AP and PLA/17AP present an amorphous residue, the ones of the composites containing the ANa clay present a high crystallinity, exhibiting the characteristic reflections of silicon phosphate ( $\text{SiP}_2\text{O}_7$ ). This is an indicative of the interaction

FIGURE 10 SEM images the internal surface of the char for each composite, with 50× magnitude



between ANa (the only source of Si) and ammonium polyphosphate (the only source of P). Only the intensity of the reflections varies among the diffractograms. The composites containing 1.2% of ANa present lower intensity than the ones with 3% of ANa. The higher intensity in the XRD reflection is associated to a higher degree of organization of the crystalline species. For the char, a higher organization can be prejudicial, implying a more brittle surface. The XRD results can be correlated to the ones of the cone calorimeter, which shows that the composites containing 3% of ANa present the poorer fire behavior. It is possible that a more fragile surface would not be able to retain the gases released during the material degradation, promoting cracks and holes on the char surface and, consequently, imparting the flame-retardant properties.

### 3.5 | Scanning electron microscopy of the composites

SEM images of the inner surface of the original composites, that is, before being burnt, and the internal and external surfaces of the residual char after burn are shown in Figures 8-10. The neat PLA (Figure 8) presents

a smooth and plain surface, in contrast with the rough and hilly surfaces of the composites. It is possible to identify the white nodular particles of ammonium polyphosphate (AP) and the dark spherical particles of lignin. The distribution of these particles in the polymeric matrix is similar in all the composites which is an indication that the differences observed in the fire-retardant properties cannot be attributed to the particle distribution of the additives.

In the Figure 9 one can observe that the morphology of the external surface of the char (i.e., the surface exposed to the heat source and to the flames) changes as a function of the ammonium polyphosphate and the clay concentrations. The PLA/16AP composite presents a rough and rugged surface, with many holes and fractures. Compared with PLA/16AP, the addition of 1.2% of ANa as in PLA/16AP/1ANa seems to improve the integrity of the char, as there is a significant reduction of fissures and holes. However, increasing the % ANa to 3% did not contribute to the char quality, as the surface presents larger holes and fractures which could entail brittleness.

The PLA/17AP surface is less rough and more homogeneous than the one of PLA/16AP, with fewer and smaller holes and cracks. After the addition of 1.2% ANa,

as in PLA/17AP/1ANa, fewer fractures are observed. PLA/17AP/3ANa shows the poorest quality char, with more fractures and holes, when compared with PLA/17AP and to PLA/17AP/1ANa. According Figure 10, the inner surface of the char has a spongy structure for all of the composites. This aspect is due to the release of gases produced during the reactions of the intumescent formulation and the degradation of the polymeric matrix. Composites without clay present larger pores in their inner surfaces when compared with the composites with clay. Moreover, the pores seem better distributed and more homogeneous in size for the composites with 1.2% of montmorillonite than for the ones with 3%. Again, PLA/17AP/1ANa presents a particular structure, probably because there are gas bubbles trapped within its pores. The better structured char presented by the composites with 1.2% of ANa in comparison to the ones with 3% can explain the differences in the curve profiles obtained in the cone calorimeter test. Also, the particular features of the PLA/17AP/1ANa system can be related to its better performance in the cone calorimeter tests.

## 4 | CONCLUSIONS

This work addressed the evaluation of the flame-retarding properties of a new formulation composed of ammonium polyphosphate, lignin and a raw montmorillonite in a PLA matrix. Overall, the concentrations of AP and montmorillonite influenced the thermal stability and the flame-retarding properties of the studied composites.

The best performance was achieved by the system containing the highest concentration of ammonium polyphosphate (17%) and the lowest montmorillonite concentration (1.2%), while keeping the concentration of lignin constant (3%). This composite showed the greatest reduction of the pHRR (53% when compared with the neat PLA), a well-structured char with the highest amount of residue in the CC test, associated to the highest LOI (39%) value and the most thermally stable products in the TGA (165% of the residue of the correspondent composite without clay, PLA/17AP). Raising the % montmorillonite to 3% seems detrimental to the fire behavior as the composite presents a higher THR value, a poor structured char, as well as an inferior thermal stability when compared with the composites containing 1.2% montmorillonite. The results obtained with his novel formulation containing APP, lignin and a raw montmorillonite can lead to the development of more sustainable and efficient flame-retardant materials.

## ACKNOWLEDGMENTS

This work was supported by CAPES (Coordenação de Aperfeiçoamento de Pessoal de Nível Superior) [001],

CNPq (Conselho Nacional de Desenvolvimento Científico e Tecnológico) [307924/2019-0], FAPERJ (Fundação Carlos Chagas Filho de Amparo à Pesquisa do Estado do Rio de Janeiro) [E-26/202.939/2017, E-26/201.861/2019, and E-26/010.002270/2019], and INOMAT (Instituto Nacional de Ciência e Tecnologia em Materiais Complexos Funcionais) [CNPq 465452/2014-0].

## AUTHOR CONTRIBUTIONS

**Raíssa Carvalho Martins:** Formal analysis (lead); investigation (lead); writing – original draft (lead). **Simone Pereira Da Silva Ribeiro:** Conceptualization (lead); methodology (lead); supervision (lead); writing – review and editing (lead). **Regina Sandra Veiga Nascimento:** Resources (lead); writing – review and editing (lead). **Marco Antonio Chaer Nascimento:** Supervision (lead); writing – review and editing (lead). **Marcos Batistella:** Methodology (supporting); writing – review and editing (lead). **José-Marie Lopez-Cuesta:** Resources (lead); supervision (lead); writing – review and editing (lead).

## DATA AVAILABILITY STATEMENT

Research data are not shared.

## ORCID

Raíssa Carvalho Martins  <https://orcid.org/0000-0002-6192-531X>

Simone Pereira da Silva Ribeiro  <https://orcid.org/0000-0003-0579-5386>

Regina Sandra Veiga Nascimento  <https://orcid.org/0000-0002-0324-1294>

Marco Antonio Chaer Nascimento  <https://orcid.org/0000-0002-5655-0576>

Marcos Batistella  <https://orcid.org/0000-0003-4002-208X>

José-Marie Lopez-Cuesta  <https://orcid.org/0000-0002-1723-3287>

## REFERENCES

- [1] W. Zhao, C. Kumar Kundu, Z. Li, X. Li, Z. Zhang, *Compos. Part A Appl. Sci. Manuf.* **2021**, *145*, 106382. <https://doi.org/10.1016/j.compositesa.2021.106382>.
- [2] F. Seidi, E. Movahedifar, G. Naderi, V. Akbari, F. Ducos, R. Shamsi, H. Vahabi, M. R. Saeb, *Polymer* **2020**, *12*, 1701. <https://doi.org/10.3390/POLYM12081701>
- [3] H. Vahabi, L. Michely, G. Moradkhani, V. Akbari, M. Cochez, C. Vagner, E. Renard, M. R. Saeb, V. Langlois, *Materials* **2019**, *12*, 1. <https://doi.org/10.3390/ma12142239>.
- [4] A. Gallos, G. Fontaine, S. Bourbigot, *Polym. Adv. Technol.* **2013**, *24*, 130. <https://doi.org/10.1002/pat.3058>.
- [5] Y. Ding, M. B. McKinnon, S. I. Stolarov, G. Fontaine, S. Bourbigot, *Polym. Degrad. Stab.* **2016**, *129*, 347. <https://doi.org/10.1016/j.polymdegradstab.2016.05.014>.

- [6] A. Regazzi, M. F. Pucci, L. Dumazert, B. Gallard, S. Buonomo, R. Ravel, J. M. Lopez-Cuesta, *Polym. Degrad. Stab.* **2019**, *163*, 143. <https://doi.org/10.1016/j.polymdegradstab.2019.03.008>.
- [7] K. Wu, Y. Hu, L. Song, H. Lu, Z. Wang, *Ind. Eng. Chem. Res.* **2009**, *48*, 3150. <https://doi.org/10.1021/ie801230h>.
- [8] Y. Guo, C. C. Chang, M. A. Cuiffo, Y. Xue, X. Zuo, S. Pack, L. Zhang, S. He, E. Weil, M. H. Rafailovich, *Polym. Degrad. Stab.* **2017**, *137*, 205. <https://doi.org/10.1016/j.polymdegradstab.2017.01.019>.
- [9] F. D. Sypaseuth, E. Gallo, S. Çiftci, B. Schartel, *e-Polymers* **2017**, *17*, 449. <https://doi.org/10.1515/epoly-2017-0024>.
- [10] H. Zhu, Q. Zhu, J. Li, K. Tao, L. Xue, Q. Yan, *Polym. Degrad. Stab.* **2011**, *96*, 183. <https://doi.org/10.1016/j.polymdegradstab.2010.11.017>.
- [11] H. Nishida, Y. Fan, T. Mori, N. Oyagi, Y. Shirai, T. Endo, *Ind. Eng. Chem. Res.* **2005**, *44*, 1433. <https://doi.org/10.1021/ie049208+>.
- [12] D. M. Fox, J. Lee, C. J. Citro, M. Novy, *Polym. Degrad. Stab.* **2013**, *98*, 590. <https://doi.org/10.1016/j.polymdegradstab.2012.11.016>.
- [13] C. Réti, M. Casetta, S. Duquesne, S. Bourbigot, R. Delobel, *Polym. Adv. Technol.* **2008**, *19*, 628. <https://doi.org/10.1002/pat.1130>.
- [14] R. Zhang, X. Xiao, Q. Tai, H. Huang, Y. Hu, *Polym. Eng. Sci.* **2012**, *52*, 2620. <https://doi.org/10.1002/pen.23214>.
- [15] V. Carretier, J. Delcroix, M. F. Pucci, P. Rublon, J. M. Lopez-Cuesta, *Materials* **2020**, *13*, 2450. <https://doi.org/10.3390/ma13112450>
- [16] A. Cayla, F. Rault, S. Giraud, F. Salaün, V. Fierro, A. Celzard, *Polymers* **2016**, *8*, 331. <https://doi.org/10.3390/polym8090331>
- [17] X. Jin, X. Gu, C. Chen, W. Tang, H. Li, X. Liu, S. Bourbigot, Z. Zhang, J. Sun, S. Zhang, *J. Mater. Sci.* **2017**, *52*, 12235. <https://doi.org/10.1007/s10853-017-1354-5>.
- [18] L. Ferry, G. Dorez, A. Taguet, B. Otazaghine, J. M. Lopez-Cuesta, *Polym. Degrad. Stab.* **2015**, *113*, 135. <https://doi.org/10.1016/j.polymdegradstab.2014.12.015>.
- [19] G. Fontaine, S. Bourbigot, *J. Appl. Polym. Sci.* **2009**, *113*, 3860. <https://doi.org/10.1002/app.30379>.
- [20] G. Fontaine, A. Gallos, S. Bourbigot, *Fire Saf. Sci.* **2014**, *11*, 808. <https://doi.org/10.3801/IAFSS.FSS.11-808>.
- [21] R. C. Martins, M. J. C. Rezende, M. A. C. Nascimento, R. S. V. Nascimento, S. P. Ribeiro, *Polymers* **2020**, *12*, 2781. <https://doi.org/10.3390/polym12122781>.
- [22] S. Bourbigot, M. Le Bras, P. Bréant, J.-M. Trémillon, R. Delobel, *Fire Mater.* **1996**, *20*, 145. [https://doi.org/10.1002/\(SICI\)1099-1018\(199605\)20:3<145::AID-FAM569>3.0.CO;2-L](https://doi.org/10.1002/(SICI)1099-1018(199605)20:3<145::AID-FAM569>3.0.CO;2-L).
- [23] G. Chigwada, C. A. Wilkie, *Polym. Degrad. Stab.* **2003**, *81*, 551. [https://doi.org/10.1016/S0141-3910\(03\)00156-3](https://doi.org/10.1016/S0141-3910(03)00156-3).
- [24] R. Zhang, X. Xiao, Q. Tai, H. Huang, J. Yang, Y. Hu, *J. Appl. Polym. Sci.* **2013**, *127*, 4967. <https://doi.org/10.1002/app.38095>.
- [25] S. Bourbigot, S. Duquesne, *J. Mater. Chem.* **2007**, *17*, 2283. <https://doi.org/10.1039/b702511d>.
- [26] S. P. S. Ribeiro, R. C. Martins, L. S. Cescon, L. R. Estevão, M. Nascimento, *J. Appl. Polym. Sci.* **2019**, *136*, 48053. <https://doi.org/10.1002/app.48053>.
- [27] M. Herrera, G. Matuschek, A. Kettrup, *J. Therm. Anal. Calorim.* **2000**, *59*, 385. <https://doi.org/10.1023/A:1010177105297>.
- [28] W. Xi, L. Qian, Y. Qiu, Y. Chen, *Polym. Adv. Technol.* **2016**, *27*, 781. <https://doi.org/10.1002/pat.3714>.
- [29] G. Tang, R. Zhang, X. Wang, B. Wang, L. Song, Y. Hu, X. Gong, *Macromol. Sci. Part A Pure Appl. Chem.* **2013**, *50*, 255. <https://doi.org/10.1080/10601325.2013.742835>.
- [30] Lactic acid, NIST Stand. Ref. Database 69 NIST Chem. Webb. (accessed 42321) **2018**.
- [31] S. Inkinen, M. Hakkarainen, A. C. Albertsson, A. Södergård, *Biomacromolecules* **2011**, *12*, 523. <https://doi.org/10.1021/bm101302t>.
- [32] G. Gorrasi, R. Pantani, *Adv. Polym. Sci.* **2017**, *279*, 119. [https://doi.org/10.1007/12\\_2016\\_12](https://doi.org/10.1007/12_2016_12).
- [33] D. L. Pavia, G. M. Lampman, G. S. Kriz, J. R. Vyvyan, *Introduction to spectroscopy*, 5th ed., Cengage Learning, Stamford, Connecticut **2015**.
- [34] S., Bourbigot, M. Le Bras, R. Delobel, P. Bréant, J. M. Trémillon, Carbon N. Y. **1995**, *33*, 283. [https://doi.org/10.1016/0008-6223\(94\)00131-I](https://doi.org/10.1016/0008-6223(94)00131-I)
- [35] C. Chen, X. Gu, X. Jin, J. Sun, S. Zhang, *Carbohydr. Polym.* **2017**, *157*, 1586. <https://doi.org/10.1016/j.carbpol.2016.11.035>.
- [36] J. Zhan, L. Song, S. Nie, Y. Hu, *Polym. Degrad. Stab.* **2009**, *94*, 291. <https://doi.org/10.1016/j.polymdegradstab.2008.12.015>.
- [37] S. P. S. Ribeiro, L. R. M. Estevão, C. M. C. Pereira, R. S. V. Nascimento, *J. Appl. Polym. Sci.* **2013**, *130*, 1759. <https://doi.org/10.1002/app.39349>.